WIDEBAND DUAL-POLARIZED ELEMENT FOR A PHASED ARRAY

by
Alfred R. Lopez
Hazeltine Corporation
Wheeler Laboratory
Greenlawn, N. Y. 11740

To be presented at
Twenty-Third Annual Symposium
USAF Antenna Research and Development
October 1973

I. Introduction.

Phased-array antenna technology continues to develop; presently much interest and effort is directed toward increasing scan capability, frequency bandwidth and polarization versatility. The development of array antennas with increased coverage is restricted by the inherent limitations of the radiating element. This paper presents the results of a study which explores the capability and practicality of an aperture-element configuration for maximizing the coverage of angle, frequency, and polarization.

The initial results of this study have been encouraging. Two major milestones in the development of a wideband dual-polarized element have been: (1) the statement of the fundamental difference between the bandwidth capability of a small element in an active array and the capability of the same element when it operates in an isolated environment, and (2) the recognition that the thin "high-k" dielectric sheet, which has been used for wide-angle impedance matching [1], also provides wide-frequency impedance matching or increased bandwidth capability.

One remaining problem for the wideband dual-polarized element is the design of a practical method for realizing the bandwidth capability of the basic element configuration. This involves the coupling of wideband (TEM-coaxial) element ports to the aperture-cavity circuit. Some progress in this area has been achieved.

II. Design Objectives and Approach.

The design objectives for the dual-polarized phased-array antenna are a 2:1 (67%) bandwidth with a VSWR < 3 and an angle coverage corresponding to a 120° cone. Extension of coverage to hemispherical is a secondary objective; for the additional coverage region, dual polarization is not required. Figure 1 presents

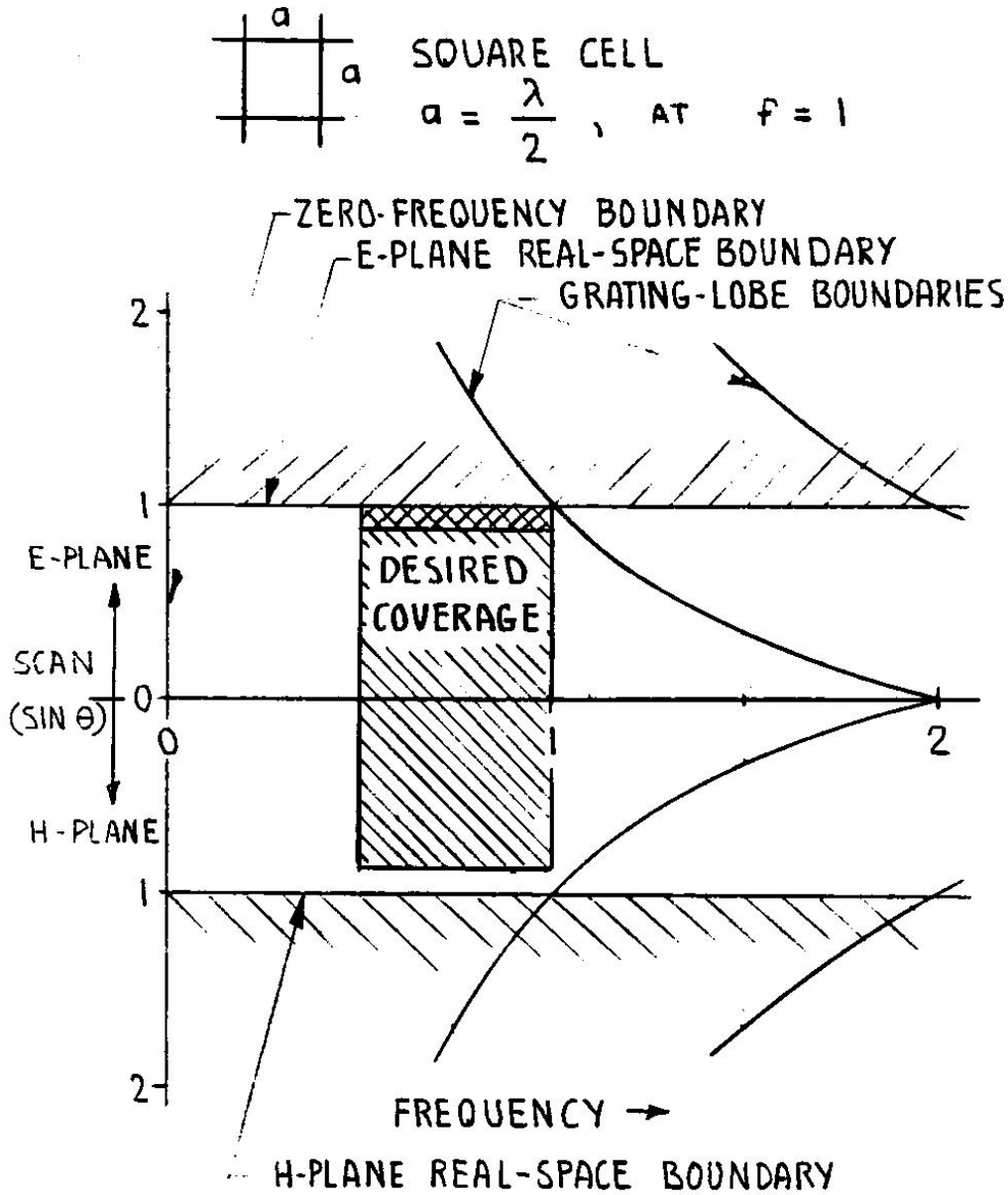

FIGURE 1. FREQUENCY-ANGLE COVERAGE CHART FOR DISPLAYING PHASED ARRAY CHARACTERISTICS.

the desired frequency-angle coverage on a chart where the E- and H-plane scan angles are plotted as one coordinate. (This chart provides a means for displaying phased-array characteristics as a function of frequency and the principal scan angles.)

To meet the design objectives, certain restrictions are imposed on the element-aperture parameters. Dual polarization, for practical purposes, requires that the element be either a square or a circle. Also, a square grid for the elements guarantees the same performance for the two nominally crossed-polarized signals in two perpendicular scan planes; this results in some simplification in the array design. As noted in Figure 1, certain inherent boundaries, where unity reflection occurs, restrict the frequency-angle coverage. At the highest frequency, grating-lobe effects limit the element spacing to less than a half wavelength. Consequently, the element configuration is restricted to a square pipe below cutoff. The square pipe can be terminated with a short circuit, not too close to the aperture, to form a relatively shallow cavity.

Figure 2 summarizes the objectives, considerations, and the related aperture design parameters for the wideband dual-polarized array. As indicated in the figure, the wideband performance is related to a large radiation power factor (the ratio of radiated-to-reactive power that is characteristic of the aperture). For small elements, the larger the element the larger is the power factor. As a result, the basic element configuration is a thin-walled square-pipe cavity which varies from a quarter wavelength on a side at the lowest frequency to a half wavelength at the highest frequency. A thin "high-k" dielectric window is used for tuning to resonance; the window is needed for realizing the power factor.

OBJECTIVE	CONSIDERATIONS	ELEMENT DESIGN FACTORS
DUAL POLARIZATION	SIMILAR PERFORMANCE IN TWO ⊥ SCAN PLANES	SHAPE GRID
WIDEBAND	LARGE RADIATION POWER FACTOR (LARGE CONDUCTANCE AND SMALL INTERNAL AND EXTERNAL SUSCEPTANCE)	SIZE TYPE
WIDEANGLE	SMALL VARIATION OF CONDUCTANCE AND SUSCEPTANCE AVOID RESONANCE OR SURFACE-WAVE EFFECTS	SPACING

FIGURE 2. DESIGN APPROACH FOR WIDEBAND DUAL-POLARIZED PHASED ARRAY APERTURE

III. Basic Principles for Wideband Operation.

Two principles form the basis for predicting that the design objectives given above for the wideband dual-polarized element can be met. The first is the rule for the bandwidth dependence on the cell size and scan, and the second describes the increased bandwidth capability of an aperture with a thin "high-k" dielectric sheet spaced in front of it.

A. Bandwidth Dependence on Cell Size and Scan.

The array element being considered can be viewed as a small antenna which radiates in only one direction at a time, as contrasted with the usual small antenna which radiates in all directions simultaneously. The rules for the bandwidth capability of small antennas are well known [2]. In general, the bandwidth for a small antenna is proportional to a volume ratio or to $(a/\lambda)^3$ where "a" is the side of an equivalent cube. This rule is not valid for the active phased-array case; the bandwidth capability of a small element in the active phased-array environment is much greater than the bandwidth of the same element when it is operating as an isolated element.

The bandwidth capability of an antenna is directly proportional to its radiation power factor (PF). An approximation for the power factor of the element being considered, when it is operating as an isolated element, is given in Figure 3. As shown in the figure, the power factor evaluated near mid frequency is about 0.15. Using the rules as stated by Fano for broadband matching of arbitrary impedances [3][4], it is determined that a 40% bandwidth is practical for a VSWR < 3; this assumes a double-tuning technique. The theoretical upper bound for an infinite number of tuned circuits is 63%. Therefore, the indications are that the isolated element does not have the capability for achieving the bandwidth design objective of 67%.

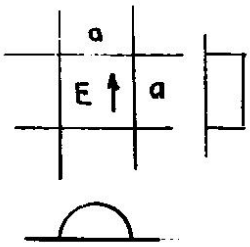

TE-10 MODE

SQUARE PIPE TUNED TO RESONANCE BY THIN "HIGH k" DIELECTRIC WINDOW

$$a < \frac{\lambda}{4}$$

	ELEMENT IN ACTIVE ARRAY		ISOLATED ELEMENT
	BROADSIDE	60° H-PLANE	
RADIATION G	$\frac{4}{\pi^2}$	$\frac{2}{\pi^2}$	$\frac{16}{3\pi}\left[\frac{a}{\lambda}\right]^2$
EXTERNAL B_x	$-\frac{1}{\pi^2}\frac{\lambda}{a}$		$-.16\frac{\lambda}{a}$
WINDOW B_w	$-\left[B_x + B_i\right]$		
CAVITY B_i	$-\frac{1}{4}\frac{\lambda}{a}$		
POWER FACTOR $PF = \frac{G}{B_x + B_i}$	$1.2\frac{a}{\lambda}$	$0.6\frac{a}{\lambda}$	$4\left[\frac{a}{\lambda}\right]^3$
PF $\left[\frac{a}{\lambda} = \frac{1}{3}\right] \approx$	0.4	0.2	0.15

FIGURE 3. POWER FACTOR FORMULAS

The power factor for the element in the active array is a function of scan angle. Figure 3 shows, for the infinite-array unit cell, the admittance values for the broadside scan condition normalized to freespace admittance. The radiation loading (conductance) depends on the cell shape but is independent of cell size; for the TE-10 mode and a square cell shape the conductance is slightly less than 1/2 that of freespace. The total inductive susceptance, or stored power (magnetic), is the sum of the reactive power for all cutoff modes in the pipe and in freespace. The important result, shown in Figure 3, is that the power factor for the element in the active array environment is proportional to the first power of the side of the square cell.

For H-plane scan, the radiation conductance decreases by a factor of 1/2 at 60° scan while the reactive power remains unchanged. The power factor, evaluated at mid frequency, is 0.2. A comparison of this power factor to that of the isolated element indicates that the element in the active array, scanned to 60° in the H-plane, has somewhat more bandwidth capability than the isolated element. However, a still higher power factor is required for a practical design to meet the objectives.

B. Increased Bandwidth with Thin "High-k" Dielectric Sheet.

Dielectric material in the region external to the array aperture has the capability for modifying the constant-reflection contours such as the natural or inherent unity-reflection boundaries shown in Figure 1. A thin "high-k" dielectric sheet, spaced in front of the aperture, has the capability for substantially improving the performance of the square-pipe-cavity element operating below cutoff.

The grating lobe series and the related radiation crater [5] are the basic concepts used in evaluating the effects of dielectric material. Figure 4 shows the element grid under consideration and the corresponding grating-lobe pattern on the "sin θ plane". The pattern shown is for the case of the basic element

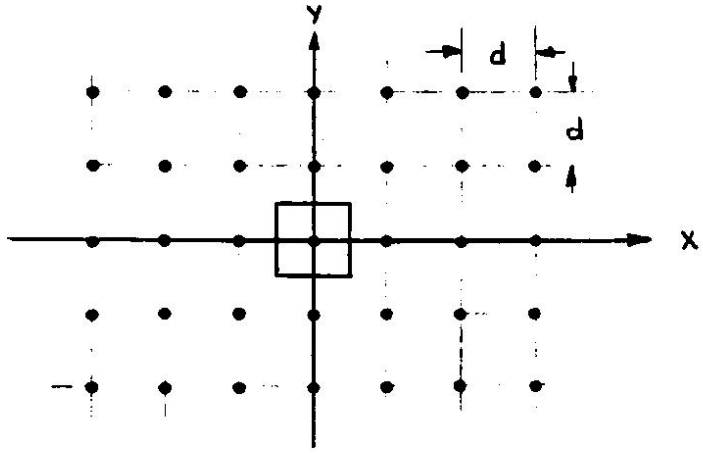

(a) ELEMENT GRID

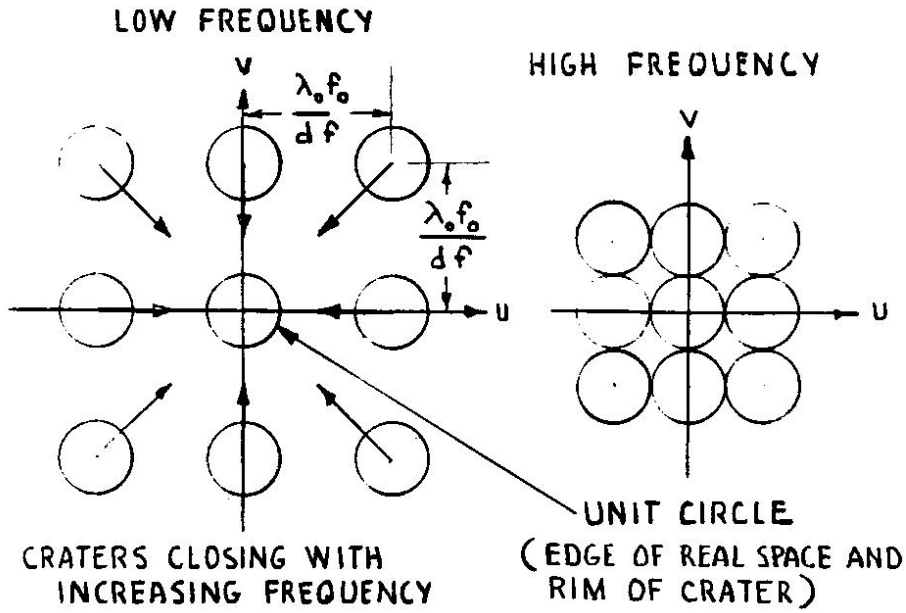

(b) RADIATION CRATERS ON "SIN θ PLANE"

FIGURE 4. GRATING LOBE SERIES WITH FREQUENCY VARIATION

without the dielectric sheet. Each circle represents the rim of a radiation crater and is centered on a grating lobe direction. The grating lobe series is a summation of all craters at a given direction in the "sin θ plane". It is observed in Figure 4 that with increasing frequency, the craters converge toward the origin.

Figure 5 shows the lumped-circuit approximation for the radiation crater for a small dipole element with a thin "high-k" dielectric sheet. It is noted that certain elements have either angle (θ) or frequency (f) dependence while others have both angle and frequency dependence. This representation has provided the basis for estimating the values of dielectric sheet thickness and spacing that result in a near optimum power factor while precluding surface-wave effects within the coverage region. The computed characteristics are given below for the cavity element with the thin "high-k" dielectric sheet. For comparison, computations for the cavity element without the dielectric sheet are also presented.

IV. Comparison of Basic Element With and Without Dielectric Sheet.

In this section a comparison of the square-pipe-cavity element with and without the thin "high-k" dielectric sheet is presented. The comparison is of computed reflection versus angle and frequency. The computations assume an infinite array, very thin cavity walls, excitation by the TE-10 mode only, and that the thin "high-k" dielectric sheet acts as a shunt capacitive susceptance. The reference terminal pair, or port, for the computations is across the face of the cavity at the interface of the cavity and freespace.

Figure 6 shows the equivalent networks for the two cases being considered. For both cases, the grating lobe series is used to compute the external admittance. For the dielectric sheet, a transmission-line transformation is used to compute the radiation or admittance crater at the reference plane.

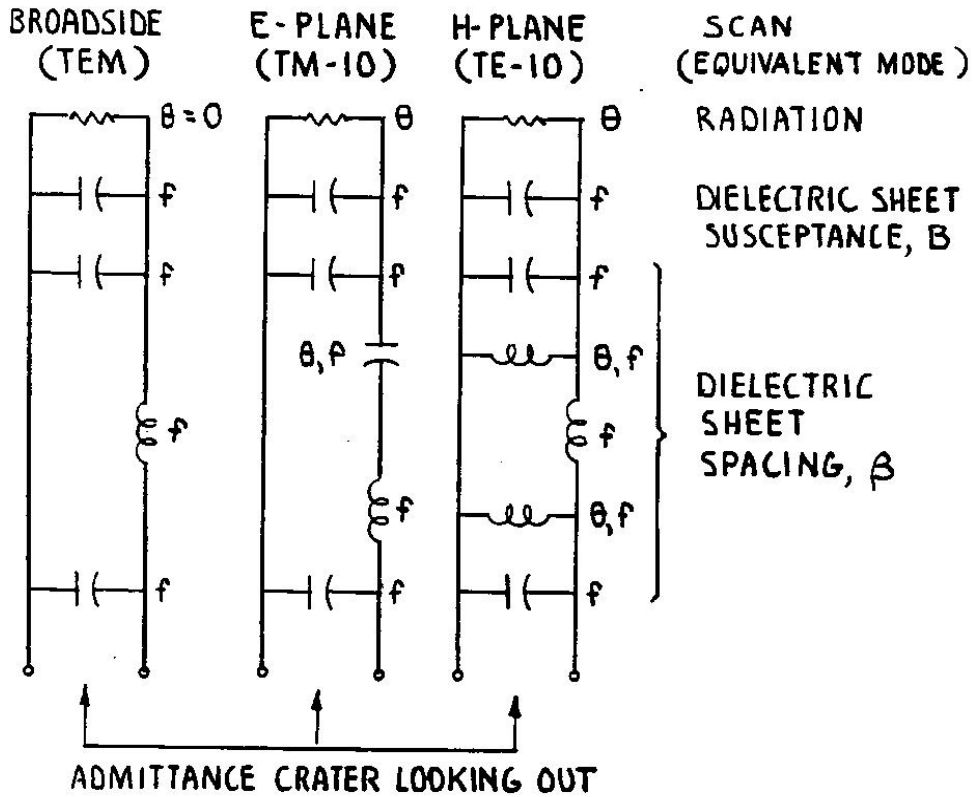

$$B = \frac{2\pi t}{\lambda}(K-1) \qquad t = \text{DIELECTRIC SHEET THICKNESS}$$

$$\beta = \frac{2\pi L}{\lambda} \qquad L = \text{DIELECTRIC SHEET SPACING}$$

B AND β SELECTED TO AVOID SURFACE-WAVE EFFECT AND TO OPTIMIZE POWER FACTOR

FIGURE 5. LUMPED CIRCUIT APPROXIMATION FOR RADIATION CRATER

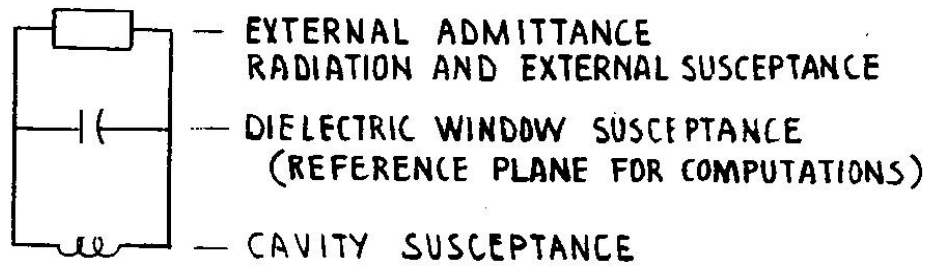

(a) WITHOUT DIELECTRIC SHEET

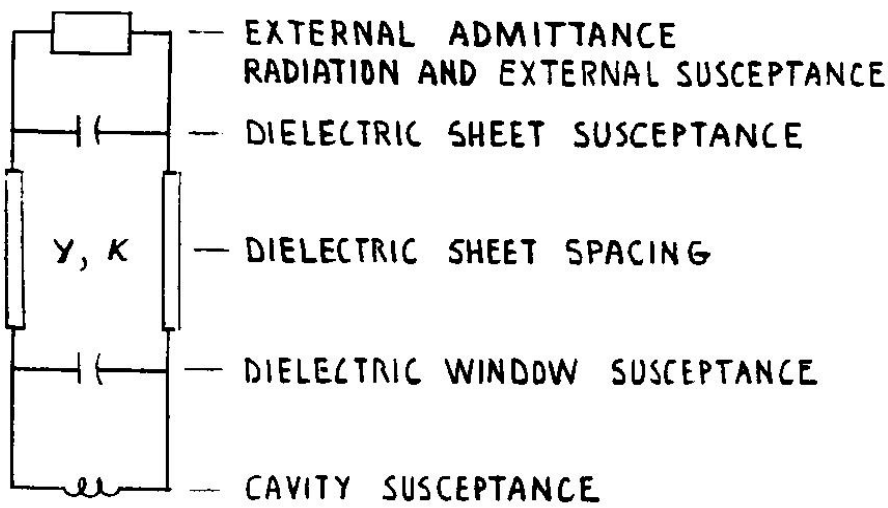

(b) WITH DIELECTRIC SHEET

FIGURE 6. EQUIVALENT CIRCUITS FOR SQUARE-PIPE-CAVITY ELEMENT

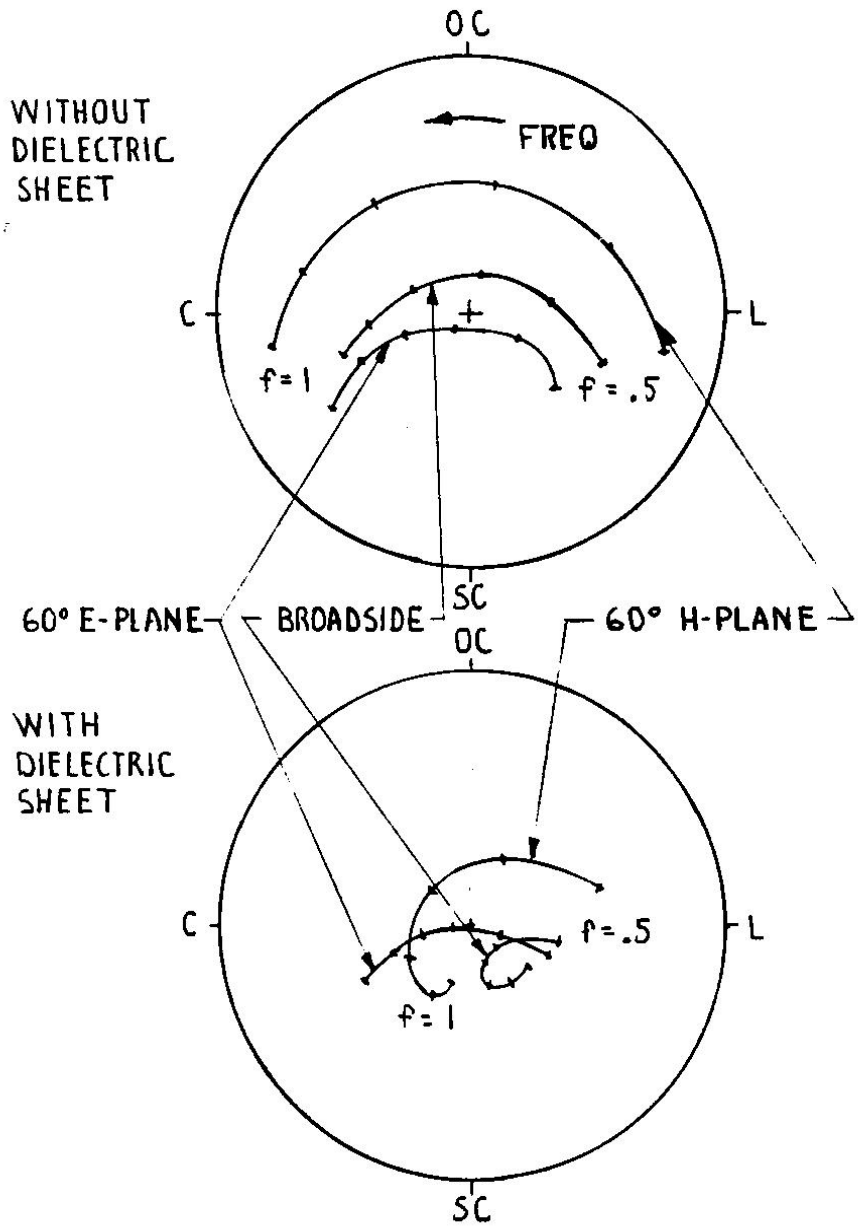

FIGURE 7. COMPUTED REFLECTION FOR SQUARE-PIPE-CAVITY ELEMENT

Figure 7 shows reflection magnitude and phase versus frequency for three scan angles, and Figure 8 shows contours of constant reflection magnitude versus frequency and angle. From both figures it is clear that the dielectric sheet substantially reduces the reflection over the desired frequency and angle coverage.

The dielectric sheet can be considered as a resonator or transformer which increases the conductance level at the cavity-freespace interface and results in improved impedance match at this surface. The important point to note is that the dielectric sheet increases the radiation power factor such that (in accordance with Fano's principle) the desired reflection tolerance and bandwidth can be achieved with a small number of tuned circuits.

V. Coupling of Element Ports and the Aperture Cavity.

So far the discussion has concentrated on the cavity-freespace interface. Computations have been made with reference to a port whose access is not easy. The problem is obtaining sufficient coupling of two wideband TEM coaxial ports with two crossed TE-10 modes in the aperture-cavity circuit. The problem is further complicated by a requirement that coupling to other modes be avoided.

Work has been done with an unbalanced configuration. The approach is shown in Figure 9; a metal-strip exciter is connected directly to the inner conductor of the coaxial port; the strip is tuned to resonance and magnetically coupled to the aperture circuit. Another strip (not shown) is located in a plane perpendicular to the paper and is connected to the cross-polarized port. Although this approach is mechanically simple, coupling to undesired modes results in a substantial degradation of performance. The inherent high radiation power factor of the basic element requires strong coupling between the exciter and

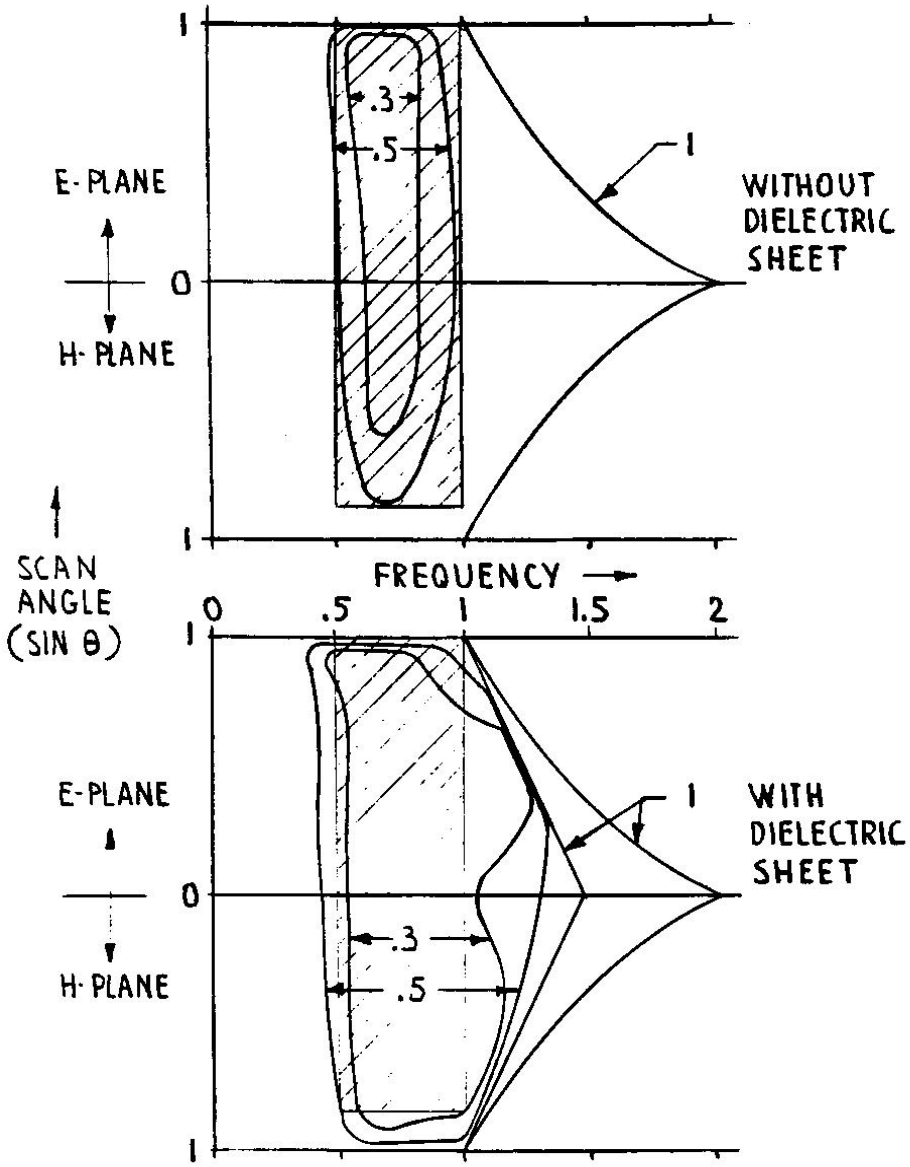

FIGURE 8. REFLECTION CONTOUR MAPS FOR SQUARE-PIPE-CAVITY ELEMENT

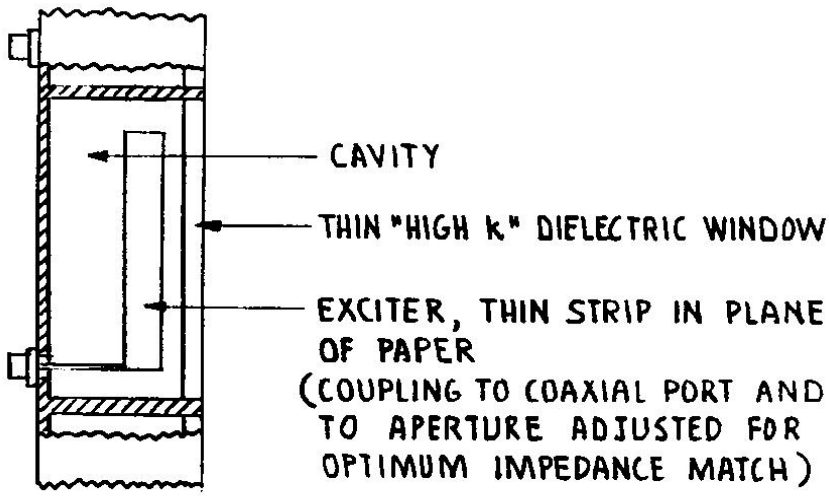

FIGURE 9. ONE METHOD FOR COUPLING THE ELEMENT PORTS TO THE APERTURE-CAVITY CIRCUIT

aperture-cavity circuit for good impedance match. It turns out that this amount of coupling is difficult to achieve without exciting undesired modes.

The results of the work done on the problem of coupling the element ports and the aperture cavity indicate that a balanced exciter configuration is required. This implies an increase in the mechanical complexity of the element in order to achieve the full bandwidth capability of the aperture-cavity circuit. Some alternatives for a balanced exciter have been considered and one approach is presently under development. The results of this work will be reported at a later date.

VI. Conclusions.

The principal conclusions for the work completed under this program are listed below:

1. The ratio of the bandwidth of a small element in the active phased-array environment to the bandwidth of the same element when it is operating as an isolated element is inversely proportional to the square of the element diameter/wavelength ratio.

2. A thin "high-k" dielectric sheet, spaced in front of the array aperture, can substantially increase the bandwidth capability of a phased array antenna with square-pipe-cavity elements below cutoff.

3. To achieve the full bandwidth capability of the square-pipe-cavity element, a symmetrical or balanced exciter section is needed to couple the element ports with the aperture-cavity circuit.

VII. Acknowledgment.

This work was performed by the Wheeler Laboratory group of the Hazeltine Corporation for the Air Force Avionics Laboratory under Contract F33615-72-C-2181. The program project engineer is John P. Shanklin of the Air Force Avionics Laboratory. Mr. Shanklin's advice and guidance contributed significantly to the progress achieved under the program. The basic principles for wideband operation of the square-pipe-cavity element, below cutoff, were first described and developed by H. A. Wheeler. This basic work has led to the continued effort to develop practical hardware for realizing the full bandwidth capability of the aperture-element configuration.

VIII. References.

[1] E. G. Magill, H. A. Wheeler, "Wide-Angle Impedance Matching of a Planar Array by a Dielectric Sheet", IEEE Trans. G-AP, Vol. AP-14, pp. 49-53; Jan. 1966. (Comments, Vol. AP-14, pp. 636-637; Sept. 1966.)

[2] H. A. Wheeler, "Fundamental Limitations of Small Antennas", Proc. IRE, Vol. 35, pp. 1479-1484; Dec. 1947. (Also see H. A. Wheeler, "Small Antennas", in this Symposium Record.)

[3] R. M. Fano, "Theoretical Limitations on the Broadband Matching of Arbitrary Impedances", Jour. Franklin Institute, Vol. 249, No. 1, pp. 57-83; No. 2, pp. 139-154; Jan.Feb. 1950.

[4] H. Jasik, "Antenna Engineering Handbook", McGraw-Hill, New York, pp. 2-46 to 2-50; 1961.

[5] H. A. Wheeler, "The Grating-Lobe Series for the Impedance Variation in a Planar Phased-Array Antenna", IEEE Trans. G-AP, Vol. AP-14, pp. 707-714; Nov. 1966.